Journal of Aeronautics, Astronautics and Aviation, Vol. 57, No. 6, pp. 1375 – 1387 (2025)
https://doi.org/10.6125/JoAAA.202506_57(6).04

Numerical Analysis of Mechanical Modifications Induced by Laser Shock Peening on AA2024-T351 for Aeronautical Structures

Sabrina Righi [1], Hamida Fekirini [1 *], Hichem Mebarki [2], Claudia Polese [3], Malika Khodja [1, 4]

[1]*Department of Mechanical Engineering, Laboratory of Mechanics and Physical Materials, Djillali Liabes University, Sidi Bel Abbes, Algeria.*
[2]*Center of Research in Mechanics (CRM), BP N73B, Freres Ferrad, Ain El Bey, Constantine, 25021-Algeria.*
[3]*School of Mechanical, Industrial & Aeronautical Engineering, University of the Witwatersrand, Johannesburg 2050, South Africa.*
[4]*Department of Materials Science and Metallurgical Engineering, University of Pretoria, Pretoria 0028 South Africa.*

ABSTRACT

This work explores the impact of Laser Shock Peening (LSP) on the mechanical state of AA2024-T351 specimens used in the aerospace industry. Numerical simulations, conducted using ABAQUS/Explicit and based on the Johnson-Cook behavior model, examine the residual stresses and plastic deformations induced by a single circular laser impact. The results reveal that LSP, with a peak pressure of 3 GPa and a pulse duration of 25.8 ns, induces surface hardening and anisotropic compressive stresses, enhancing fatigue resistance. In-depth analysis shows that damage is concentrated around the impact center, remaining below 0.03. This study highlights the importance of optimizing LSP parameters to maximize its benefits while minimizing damage, thus contributing to the improved durability of aeronautical structures.

Keywords: LSP, AA2024-T351, Johnson-Cook, Damage, Residual stress

I. INTRODUCTION

Aluminum alloys, such as 2024-T351, are widely used in the aerospace industry due to their favorable strength-to-weight ratio and good fatigue resistance [1-3]. However, for demanding applications like aircraft fuselage structures, the surface mechanical properties must be optimized to prevent crack initiation and propagation under cyclic loading. Laser Shock Peening (LSP) is a promising technique for inducing compressive residual stresses in the surface layers of materials, thereby enhancing their fatigue resistance without compromising ductility [4-6].

The LSP process relies on the use of a high-energy pulsed laser beam to generate plasma confined at the material's surface. This rapid plasma expansion creates a shock wave that hardens the surface by modifying the microstructure, inducing compressive stresses beneficial for fatigue resistance [7]. In aluminum alloys, this technique has shown significant potential to limit plastic deformations and damage, especially in areas subjected to high stresses [8].

Numerical models, particularly the Johnson-Cook behavior model, are essential for simulating and understanding the effects of LSP on materials under dynamic loads. This model accounts for the effects of stress, strain rate, and temperature, enabling realistic predictions of material responses under extreme loading conditions [9, 10]. Using material-specific parameters for AA2024-T351, the numerical model developed in this study employs ABAQUS/Explicit software to simulate the impact of a circular laser shock on a 2 mm thick specimen [11]. This simulation determines the distribution of residual stresses and plastic deformations with precision grounded in material behavior laws [12].

Manuscript received, March 6, 2025, final revision, June 3, 2025
* To whom correspondence should be addressed, E-mail: fekirini.hamida@gmail.com

LSP is particularly advantageous for aerospace applications, where structural integrity and durability are critical. By inducing compressive residual stresses, this technique reduces the risk of cracking in critical areas exposed to high fatigue cycles. Moreover, LSP does not significantly alter surface roughness, which is advantageous in contexts where strict surface finish tolerances are required [13,14]. Studies show that stress distribution is influenced by LSP parameters, such as laser pressure and pulse duration, allowing precise control over the desired mechanical effect [4,15].

Laser Shock Peening (LSP) has been widely recognized as an effective technique for enhancing the surface properties of metallic materials. A detailed review by Montross et al. [16] emphasizes the significant alterations in the mechanical behavior of metals resulting from LSP. The rapid plasma expansion induced by the laser generates a shock wave that propagates through the material, leading to deformation and an increase in compressive residual stresses near the laser-treated surface [13].

Studies have confirmed that LSP improves key surface characteristics, including hardness, fatigue resistance, wear resistance, and corrosion protection, in various metals such as titanium and magnesium alloys, stainless steel, and aluminum alloys [17-19].

Moreover, comparisons between experimental results and simulations demonstrate that the accuracy of the Johnson-Cook model is crucial for predicting stress distribution and damage under laser shock [20].

This study explores the potential of LSP in optimizing the mechanical properties of aluminum alloys by evaluating shock wave propagation effects and analyzing critical parameters to maximize the benefits of this treatment. Through robust numerical modeling, this research provides valuable insights for advanced aerospace applications, paving the way for future developments in integrating LSP into the manufacturing processes of critical components.

Aluminum alloys, such as 2024-T351, are widely used in aerospace applications due to their favorable strength-to-weight ratio and excellent fatigue resistance. However, critical structures like fuselages require optimized surface mechanical properties to prevent crack initiation and propagation under cyclic loading.

Laser Shock Peening (LSP) stands out as a promising technique by generating compressive residual stresses without compromising the material ductility. This method relies on the generation of high-pressure shock waves, which alter the microstructure of surface layers to enhance their durability. Moreover, it has been observed that the out-of-plane deformation induced by LSP increases significantly as the sample thickness decreases [21].

To better understand these effects, numerical models, particularly the Johnson-Cook behavior law, provide valuable capabilities for accurately predicting the mechanical responses of materials subjected to extreme dynamic loads. This study aims to evaluate how a single laser impact influences critical mechanical properties using a robust numerical simulation approach. The results will contribute to optimizing LSP parameters for demanding industrial applications.

Although LSP is recognized for its efficiency in enhancing material durability through the generation of residual stresses, previous studies [22-27] have shown that its parameters directly influence the distribution of these stresses. However, their impact on material damage remains underexplored. This study addresses this gap by evaluating damage, a critical factor in ensuring the durability of components subjected to high fatigue cycles, such as aerospace parts. Material damage in this context refers to the accumulation of microstructural defects (e.g., voids, dislocations) quantified by the Johnson-Cook damage parameter (D), where D = 0 indicates no damage and D = 1 represents fracture.

II. PROPERTIES OF AA2024-T351

During a laser shock process (LSP), the pressure is applied for ultra-short durations (less than 200 ns), and the surface of the material undergoes a high shock pressure (greater than 1 GPa) with a strain rate on the order of 10^6 s^{-1}.

To describe the material's constitutive behavior and its sensitivity to strain rate and/or pressure, several models have been developed.

In 1983, Johnson and Cook [28] were the first to propose an empirical relationship that accounts for the influence of temperature (T) and strain rate (ε) on the behavior of materials.

$$\sigma = \underbrace{\left[A + B\varepsilon_p^n\right]}_{\text{Elasto-plastic with hardening}} \cdot \underbrace{\left[1 + C.\ln\left(\frac{\dot{\varepsilon}}{\dot{\varepsilon}_0}\right)\right]}_{\text{Plastic strain rate}} \cdot \underbrace{\left[1 - \left(\frac{T - T_t}{T - T_f}\right)^m\right]}_{\text{Temperature effect}} \quad (1)$$

where σ is the equivalent stress and ε is the equivalent plastic strain. The material constants are A, B, n, C, and m.

A is the yield strength of the material under reference conditions, B is the strain hardening constant, n is the strain hardening exponent, C is the strain rate sensitivity coefficient, and m is the thermal softening coefficient.

The Johnson-Cook parameters for AA2024-T351 used in this study are provided in Table 1. Similarly, Young's modulus E, Poisson's ratio ν, and density ρ are the key factors influencing the elastic propagation of the shock wave in our study, as shown in Table 2.

The Johnson-Cook damage model [29] provides a cumulative damage law, there are three parts to the failure model:

$$\varepsilon_f = \underbrace{\left[D_1 + D_2 \exp\left(D_3 \exp\left(\frac{\sigma_m}{\sigma_{eq}}\right)\right)\right]}_{\text{Influence of triaxiality}} \cdot \underbrace{\left[1 + D_4 ln\left(\dot{\varepsilon}^*_p\right)\right]}_{\text{Influence of strainrate}} \cdot \underbrace{\left[1 + D_5 T^*\right]}_{\text{Influence of temperature}} \quad (2)$$

$$T^* = \frac{T - T_r}{T_m - T_r} \quad (3) \qquad D = \sum \frac{\Delta\varepsilon}{\varepsilon_f} \quad (4)$$

where D_1 to D_5 are the damage model constants, ε_f is the plastic failure strain, σ_m is the mean stress, σ_{eq} is the equivalent stress, $\dot{\varepsilon}^*_p$ is current strain rate divided by the input reference strain rate, $T*$ is the non-dimensional temperature, and T_m and T_r are the melting temperature and the room temperature, respectively.

The damage of an element is defined based on a cumulative damage law and can be represented linearly as shown below:

where $\Delta\varepsilon$ is the increment of equivalent plastic strain.

The Johnson-Cook (JC) model coupled with damage was chosen for this Laser Shock Peening (LSP) study due to its proven ability to simulate high-strain-rate deformation and progressive material failure under dynamic loading conditions like those induced by LSP. The Johnson-Cook damage parameters are presented in Table 3.

Table 1 Johnson-Cook Law Parameters for AA2024-T351

Material	A [MPa]	B [MPa]	N	m	T_f [K]	T_t[K]	C	$\dot{\varepsilon}_0$[1/s]
AA 2024-T351	369	689	0.73	1.7	775	293	0.0083	1.0

Table 2 Input Parameters for AA2024-T351 with Elastic Behavior

Material	Density ρ [g/cm^3]	Young's Modulus [MPa]	Poisson's Ratio
AA 2024-T351	2.750	72000	0.3

Table 3 Johnson-Cook Damage Parameters

D1	D2	D3	D4	D5
0.31	0.045	-1.7	0	0.005

III. NUMERICAL SIMULATION OF LASER SHOCK

The model was developed using the commercial software Abaqus [30]. An AA2024-T351 specimen with a thickness of 2 mm was modeled, subjected to a confinement pressure of 3 GPa and a laser spot diameter of 0.9 mm. Boundary conditions were carefully defined to prevent non-physical reflections—artificial wave rebounds at boundaries caused by inadequate mesh design that can distort the simulated stress fields. A fixed base ($U_1 = U_2 = U_3 = U_{R1} = U_{R2} = U_{R3} = 0$) was applied to mimic the energy absorption behavior of a large, semi-infinite specimen (Figure 1). The geometric dimensions were chosen to be sufficiently large compared to the impact zone to eliminate edge effects and wave reflections within the bulk material.

The material behavior under shock loading was assumed to follow a Johnson-Cook model coupled with damage [29]. The applied loading consisted of a quasi-instantaneous, time-varying pressure P(t) (Equation 5), with a non-uniform distribution reaching its maximum at the spherical center (Figure 2). This distribution helps reduce shear stresses at the edge of the impact zone [24].

$$P(r,t) = P(t)\sqrt{1 - 0.5\left(\frac{x^2}{R^2} + \frac{y^2}{R^2}\right)} \quad (5)$$

where P(t) is transient pressure, R is spot radius (0.45 mm), and x, y are spatial coordinates.

Figure 3 present a normalized pressure profile applied for different durations at half-maximum of the pulse (FWHM) [31]. FWHM (Full Width at Half Maximum) represents the pulse duration of the temporal pressure profile, measured at half its peak amplitude.

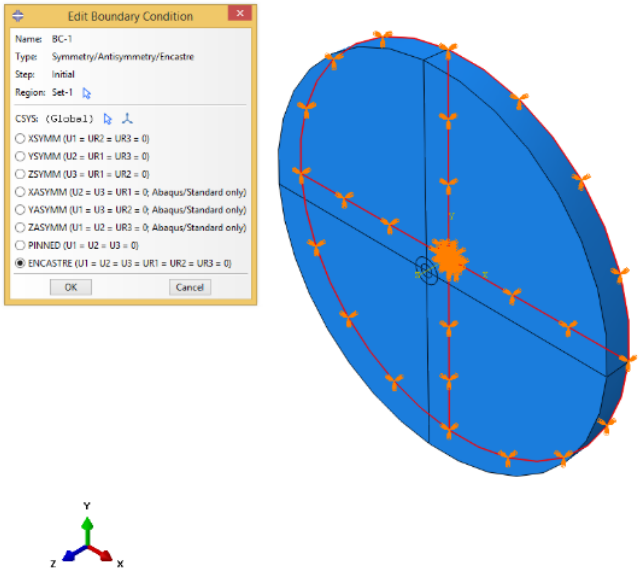

Figure 1 Boundary conditions for the specimen impacted by LSP

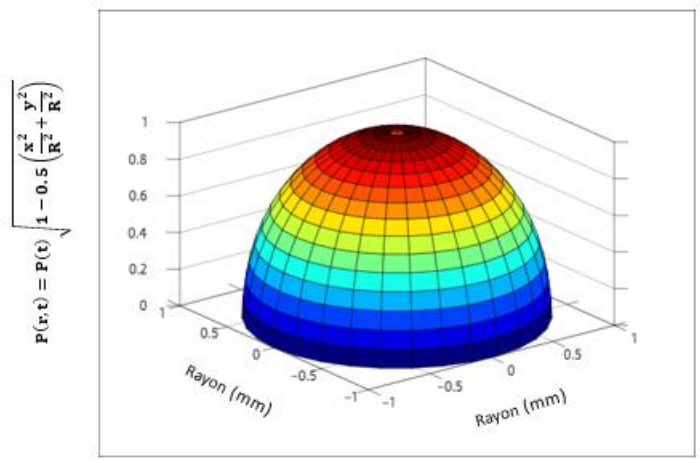

Figure 2 Quasi-spherical spatial distribution [23]

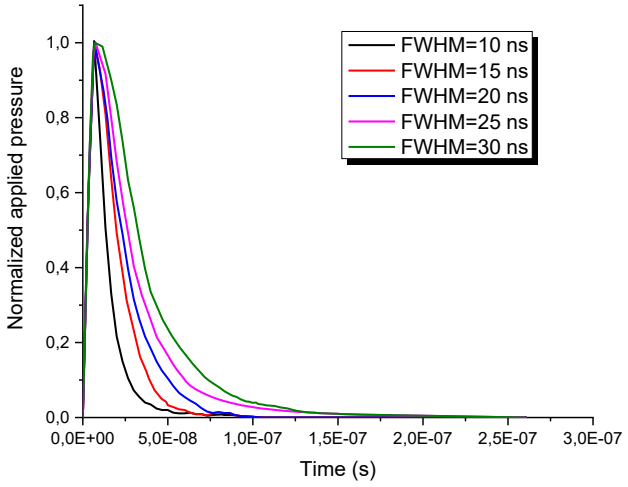

Figure 3 Normalized impact pressure-time profiles for different FWHM [31]

Fabbro et al. [32] developed an analytical formulation (Equation 2) that links the maximum pressure (expressed in GPa) to the incident laser flux.

$$P(GPa) = 0.01\sqrt{\frac{\alpha}{2\alpha+3}}\sqrt{ZI_0} \quad (6)$$

where α is the proportion of energy contributing to the pressure rise in the plasma, I_0 is the laser intensity (expressed in GW/cm²), and Z is the reduced impedance of the two materials, expressed in g·cm⁻²·s⁻¹ and given by:

$$Z = \frac{2z_1 z_2}{z_1+z_2} \quad (7)$$

Figure 4 shows the evolution of the impact pressure as a function of the laser power intensity.

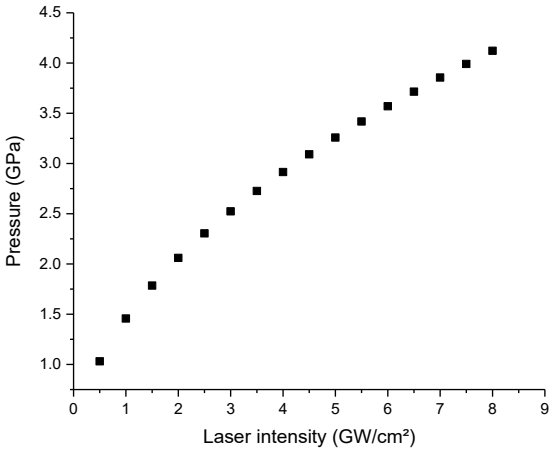

Figure 4 Evolution of pressure with laser intensity. ($\alpha \approx 0.27$, $z_{Al} = 1.5\text{x}10^6$ and $z_{water} = 0.165\text{x}10^6$)

IV. RESULTS AND DISCUSSION

4.1 Shock Wave Propagation

The laser shock process relies on concentrating a high-power pulsed laser beam (on the order of several gigawatts per square centimeter) on the surface of the materials to be treated. This results in work hardening at the surface layers, recorded as surface hardening due to microstructural changes caused by the propagation of a shock wave. These actions lead to the creation of residual stress profiles that are extremely beneficial for the fatigue resistance of mechanical components. Figures 5 and 6 illustrate the shock wave progression through the material along the x and y axes, respectively, over a period of 1000 nanoseconds. The compression gradually propagates downward and towards the edges of the treated zone. During the interaction between the laser and the material, the rapid expansion of the plasma generates uniaxial compression in the irradiated zone, along the shock wave direction, as well as expansion (stretching) of the surface layers. At the end of the laser pulse, the surrounding material reacts to the volume change and generates compressive residual stresses in the irradiated zone. These stresses are crucial for enhancing the mechanical properties, particularly the fatigue resistance of the material. A significant heterogeneity in the residual stress state at the surface was observed, which gradually decreases as one moves deeper into the subsurface. One of the key results revealed is the anisotropy of the residual stress field in most cases, where the residual stress values σ_{11} (along the primary treatment direction) are lower than the residual stress σ_{22} (perpendicular to the treatment direction).

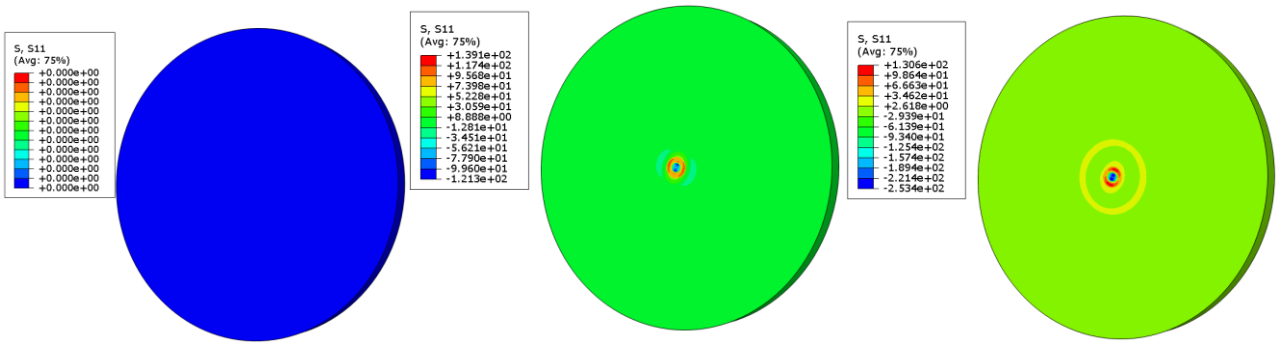

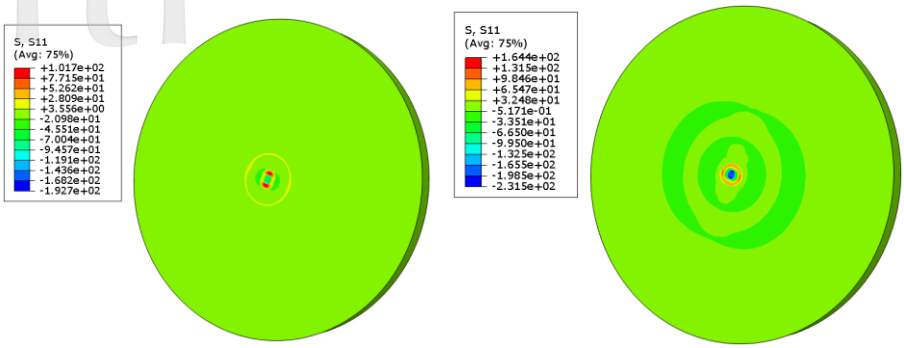

Figure 5 Propagation of the shock wave σ_{11} during the loading step (FWHM=25.8 ns, Øspot=0.9 mm, P_{max}=3 GPa)

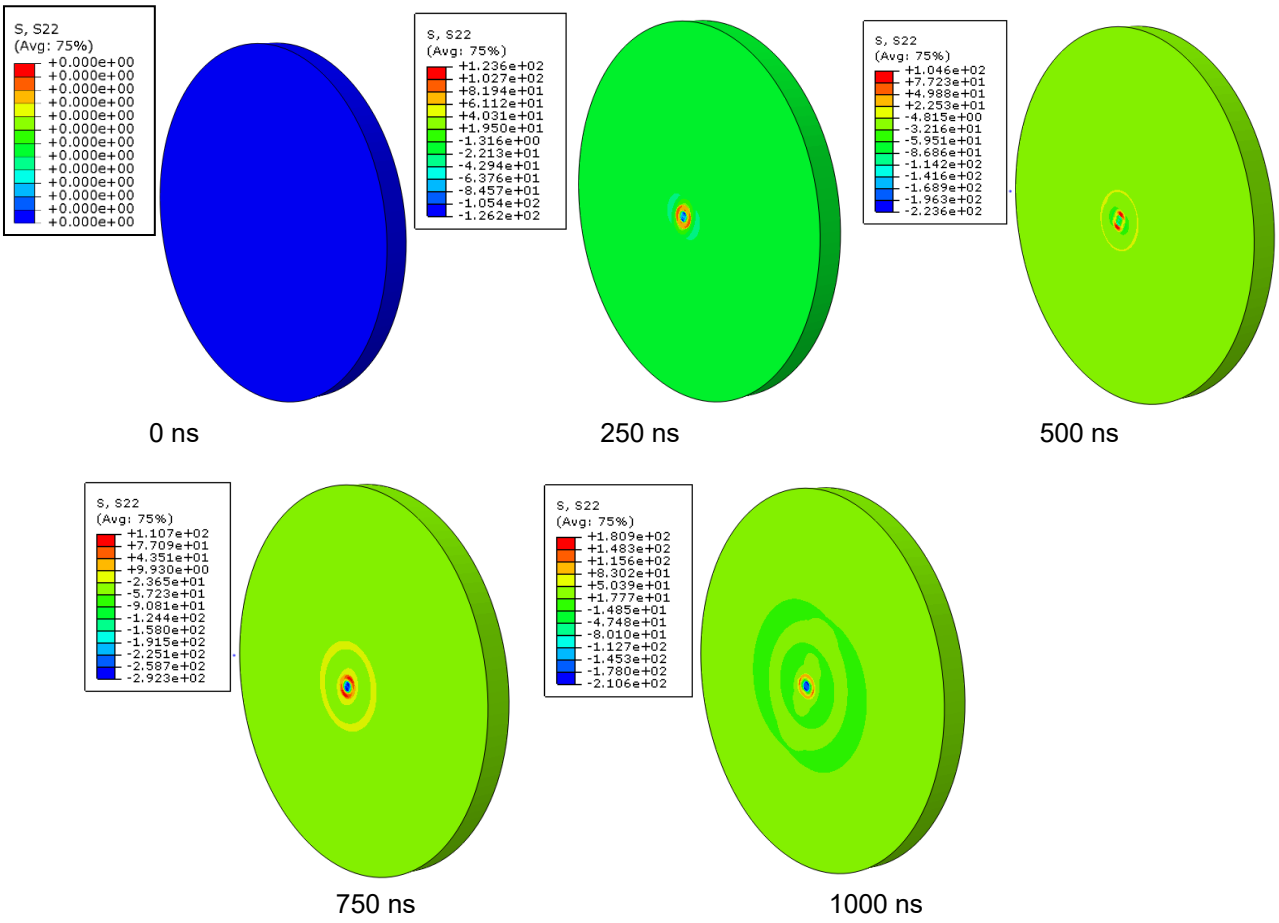

Figure 6 Propagation of the shock wave σ_{22} during the loading step (FWHM=25.8ns, Øspot = 0.9 mm, P_{max}=3 GPa)

4.2 Evolution of Johnson-Cook Damage

Considering the contribution of surface damage to fatigue behavior is crucial, as this factor can influence crack initiation. Figure 7 shows the distribution of Johnson-Cook damage over a period of 1000 ns. The maximum values are often centered around the vicinity of the laser spot center. For a single laser impact within the tolerated treatment ranges, the damage is generally less than 1. The maximum observed value is 0.027, which is achieved with the following impact parameters: FWHM=25.8 ns, Øspot=0.9 mm, P_{max}=3 GPa. Additionally, it is observed that the damage remains stable after a shock pulse duration of 250 ns.

To confirm the conclusion presented in the previous paragraph, Figure 8 illustrates the variation of Johnson-Cook damage along the X and Y spot axes. The overall damage remains very low, indicating limited material degradation. The observed asymmetry between the two

profiles is not unexpected and can be attributed to the anisotropic nature of the residual stress field and large surface stress gradients induced by the LSP process. This anisotropy is consistent with experimental observations [22,23], already investigated analytically [22,33-34], where differences in material response and shock wave propagation direction lead to slight deviations in damage distribution. The evolution of Johnson-Cook damage with depth is represented in Figure 9. It is important to note that the surface damage concentrated at the laser impact does not cause damage to the overall part. Therefore, the laser shock does not affect the internal damage of the target. For aerospace components, the JC damage model's ability to predict subcritical damage (e.g., D=0.027) ensures that LSP parameters can be optimized to enhance fatigue life without risking spallation or excessive surface degradation.

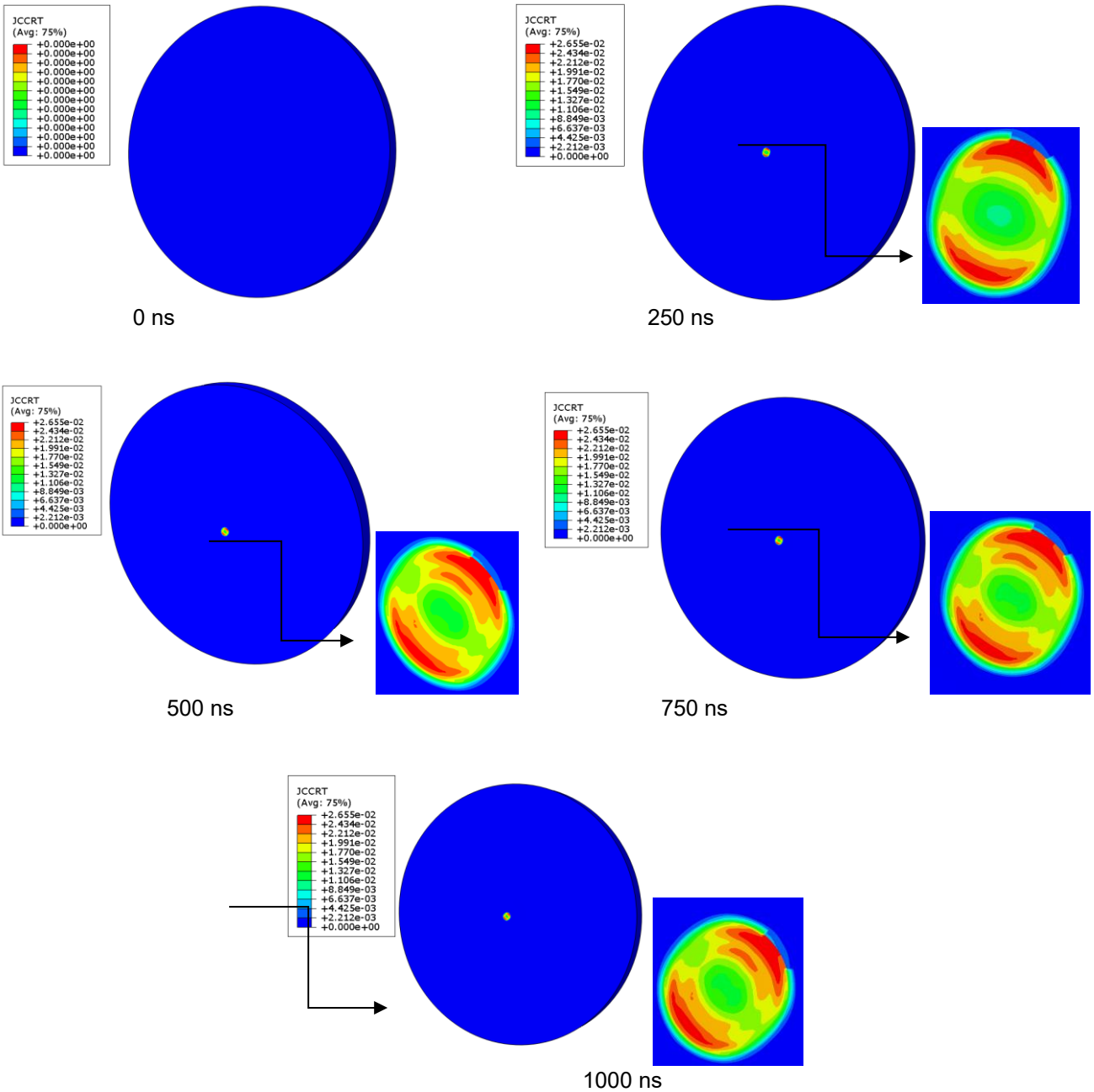

Figure 7 Johnson-Cook damage for a circular impact with the following parameters: FWHM=25.8 ns Øspot=0.9 mm, P_{max}=3 GPa

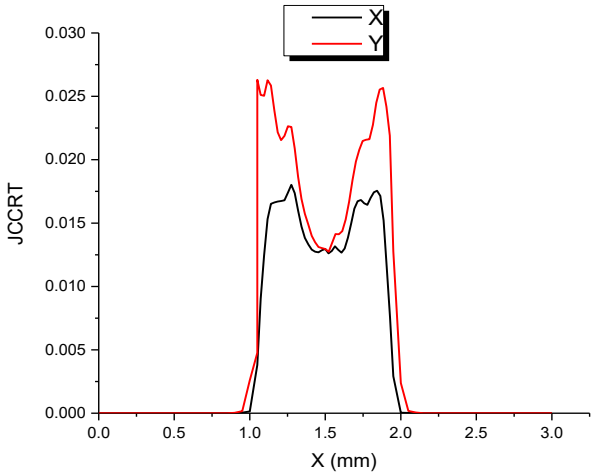

Figure 8 Damage profile with depth for a single circular impact with the following parameters: FWHM=25.8 ns, Øspot=0.9 mm, P_{max}=3 GPa

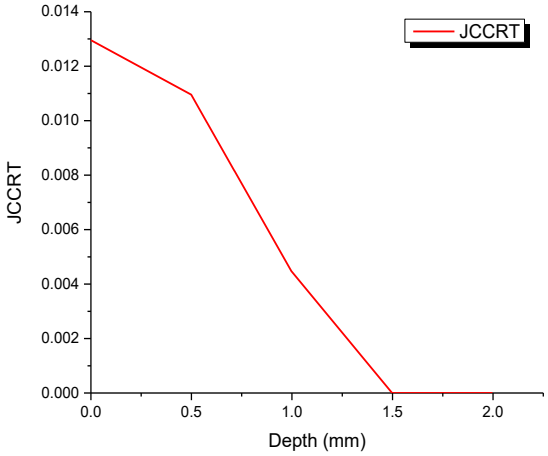

Figure 9 Damage profile with depth for a single circular impact with the following parameters: FWHM=25.8 ns, Øspot=0.9 mm, P_{max}=3 GPa

4.3 Energy Histories

Energy balance is often crucial when analyzing a material's behavior during an impact using the Abaqus/Explicit computational code [30,35]. Comparisons between the different energy components can be useful for assessing whether an analysis provides an adequate response.

During the single impact LSP process, the total external work of a pulsed pressure on the material surface is converted into kinetic energy, internal energy, and viscous energy. The history of these energies is presented in Figure 10. Kinetic energy and internal energy increase sharply to a certain value and then remain stable, gradually approaching 0.18 mJ and 3.32 mJ, respectively, while the dissipated viscous energy increases significantly and eventually stabilizes at around 0.65 mJ.

Internal energy includes both elastically stored energy and plastically dissipated energy. Figure 11 shows how the total internal energy from the different modes changes as the shock waves propagate through the treated material. The plastically dissipated energy increases significantly over a period of 300 ns and remains stable at 1.5 mJ, while the elastically stored energy gradually decreases from 2 mJ to 1 mJ after 1000 ns. Elastic energy decreases as residual stresses relax, while plastic energy stabilizes once yielding completes (~300 ns). The saturation of plastically dissipated energy implies that no further plastic deformation occurs in the material after a dissolution time of 1000 ns (energy saturation indicates plastic deformation cessation after 1000 ns).

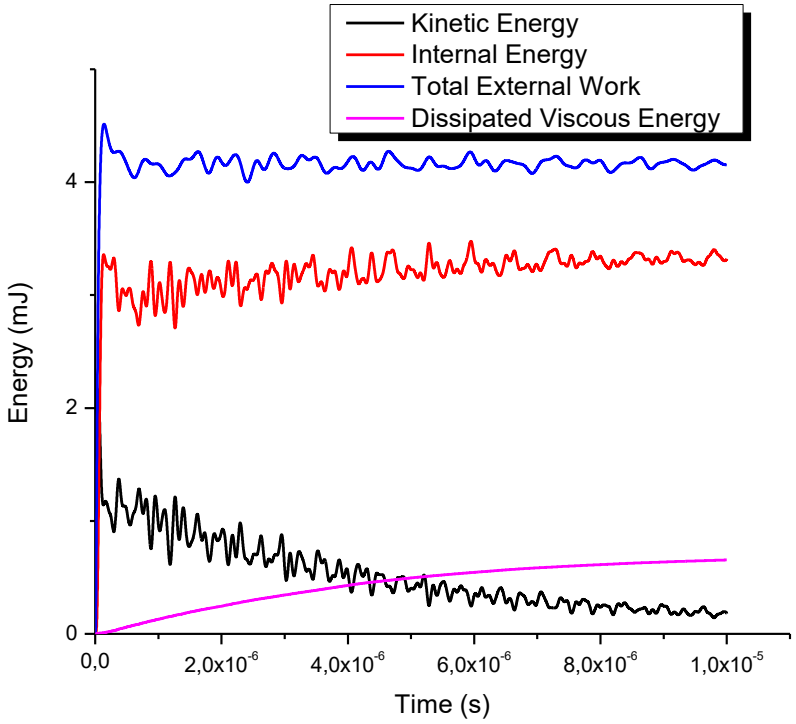

Figure 10 History of total external work, internal energy, kinetic energy, and dissipated viscous energy during the process

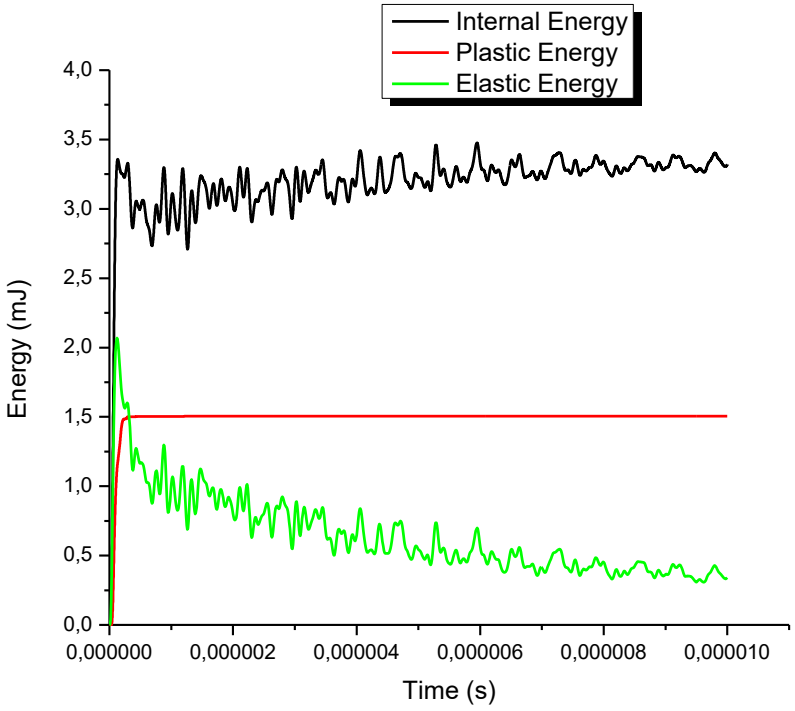

Figure 11 History of internal energy, plastic energy, and elastic energy

4.4 Surface Indentation

In general, the laser shock does not significantly alter the initial roughness of the treated material. In reality, rather than roughness, the shocked surface exhibits a waviness due to the indentation of the material subjected to the shock wave.

The formation of residual stresses induced by LSP occurs in two stages:

The material undergoes uniaxial indentation during the laser-material interaction.

After the pulse dissipates, compressive stresses are created around the impacted volume.

An example of an experimental/simulation comparison of material indentation is presented in Figures 12.a and 12.b. Figure 13 shows the evolution of surface deformation (indentation) along the X and Y axes of the spot in our numerical simulation under the following conditions: FWHM = 25.8 ns, spot diameter = 0.9 mm, P_{max} = 3 GPa. Whether considering the indentation values, the general shape of the profiles, or the height of the bulges, this result allows us to validate our model. Based on Figure 13, we can assert that the shock is asymmetric.

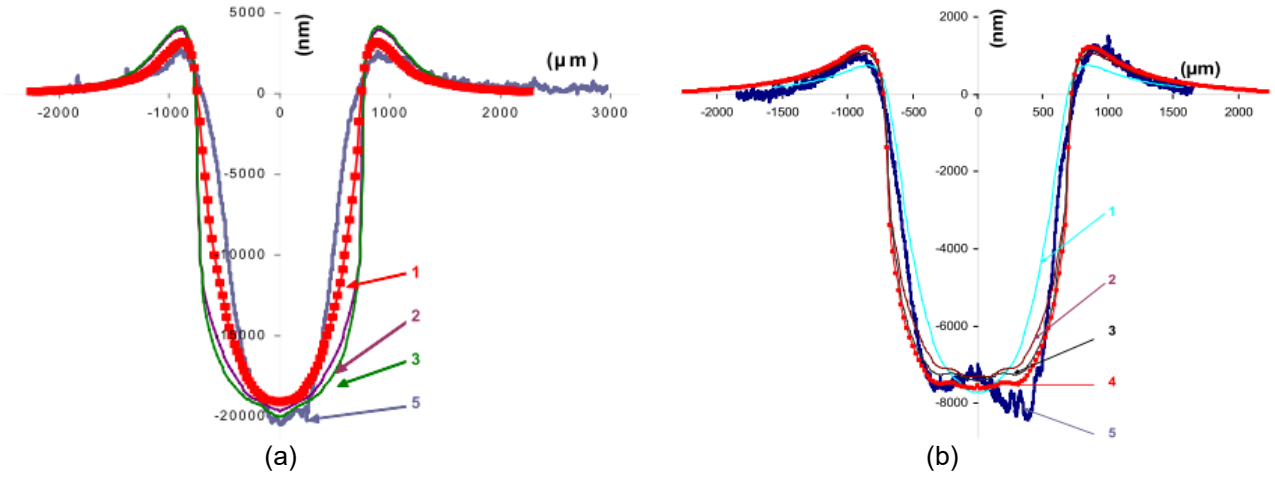

Figure 12 (a) Simulation of a laser impact on 6056-T4 (6-7 GW/cm² = 4 GPa) with different spatial distributions, (b) simulation of a laser impact (7 GW/cm² = 4.5 GPa) on 2050-T8. Curves 1 to 4 are obtained with different pressure profiles. Curve number 5 is obtained by profilometry [23]

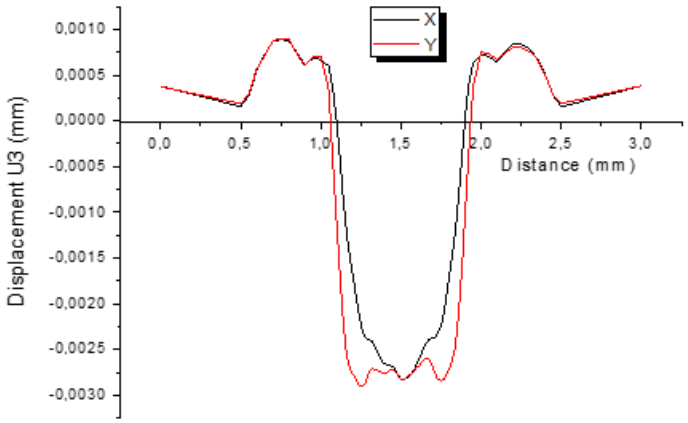

Figure 13 Evolution of surface indentation along the two axes of the impact

4.5 Plastic Deformation

When the peak pressure of the shock wave exceeds the dynamic elastic limit of the treated material, it induces extensive plastic deformation in the metal. This deformation directly results from the residual stresses. Figure 14 shows the variation in equivalent plastic deformation (PEEQ) for a single impact. It is observed that the maximum amplitude of plastic deformation is located near the surface treated by the laser shock.

The Johnson-Cook model has proven effective in capturing the mechanical responses under laser shock, particularly by predicting high strain rates and a realistic distribution of residual stresses.

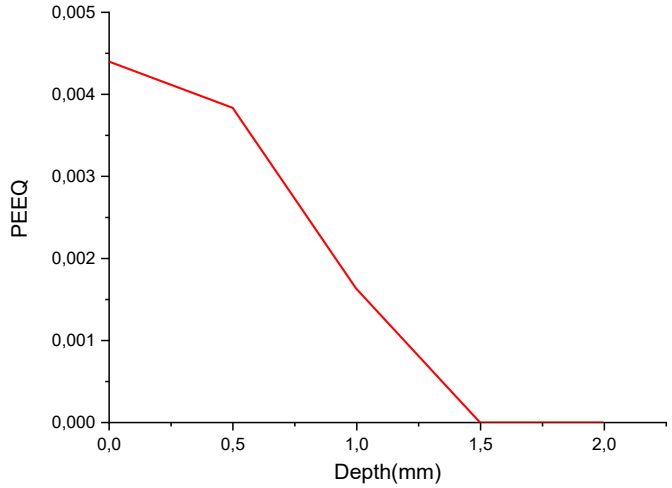

Figure 14 Equivalent plastic deformation profile in depth

V. CONCLUSIONS

This work demonstrated the significant impact of Laser Shock Peening (LSP) on the mechanical state of AA2024-T351 specimens, representing aerospace structures. Numerical simulations quantified the residual stresses and characterized the plastic deformations induced by LSP. The results indicate that the application of a single circular laser shock leads to surface hardening and the formation of anisotropic compressive residual stresses, enhancing fatigue resistance while limiting damage to negligible levels (< 0.03).

The study highlighted the importance of optimizing LSP parameters, such as power and pulse duration, to maximize mechanical benefits while minimizing material damage. The use of the Johnson-Cook model to simulate the material behavior proved effective in predicting the complex mechanical responses during treatment.

The findings provide clear recommendations for optimizing LSP parameters, ensuring improved structural integrity for critical aerospace components. They also pave the way for future research exploring the effects of LSP on other aluminum alloys and integrating this technique into advanced manufacturing processes for aerospace structures. In conclusion, LSP represents a strategic opportunity to enhance the durability and performance of mechanical components across the aerospace industry and beyond.

While this study provides promising results, it is limited to a single laser impact. Future studies should investigate the effects of multiple impacts and incorporate experimental validations to confirm these numerical predictions.

REFERENCES

[1] Shuange Shuang Li, Xin Y, QingeYuan Li, HeeLi P, BaieXin D, TianeShu L, HongeYu Y, Jun F, ShieLi S, Feng Q, Qie Chuan J, “Development and applications of aluminum alloys for aerospace industry,” *Journal of Materials Research and Technology*, Vol. 27, 2023, pp. 944-983. https://doi.org/10.1016/j.jmrt.2023.09.274

[2] Ahmad HAK, Wahyu K, Nik Rozlin NMM,Fuad SK, “Corrosion Effects on Low Cycle Fatigue (LCF) Life of Aluminum 2024-T3,” *Journal of Aeronautics, Astronautics and Aviation*, Vol. 57, No. 3S, 2025, pp. 479-484. https://doi.org/10.6125/JoAAA.202503_57(3S).19

[3] Rodopoulos CA, Curtis SA, de los Rios ER, SolisRomero J, “Optimisation of the fatigue resistance of 2024-T351 aluminium alloys by controlled shot peening methodology, results and analysis,” *International Journal of Fatigue*, Vol. 26, 2004, pp. 849-856. https://doi.org/10.1016/j.ijfatigue.2004.01.003

[4] Xiaodie C, Jiali W, Guisheng Z, Jiajun W, Xinhui C, “Laser Shock Peening: Fundamentals and Mechanisms of Metallic Material Wear Resistance Improvement,” Materials, Vol. 17, No. 4, 2024, 909. https://doi.org/10.3390/ma17040909

[5] Sara T, Enrico T, “Effect of Laser Shock Peening on the Fatigue Behavior of Thin Aluminum Panels,” *Materials Today*, Vol. 2, 2015, pp. 5006-5014. https://doi.org/10.1016/j.matpr.2015.10.090

[6] Jiayang L, Xing S, Yongjun W, Xia H, Yuansong Z, Junbiao W, “Research on the residual stress induced by square-spot laser shock peening on 2024-T351 specimens,” *International Journal of Lightweight Materials and Manufacture*, Vol. 7, 2024, pp. 849-859.

https://doi.org/10.1016/j.ijlmm.2024.06.005
[7] Xinlei P, Xiang Li, Liucheng Z, Xiaotai F, Sihai L, Weifeng H, "Effect of Residual Stress on S–N Curves and Fracture Morphology of Ti6Al4V Titanium Alloy after Laser Shock Peening without Protective Coating," *Materials,* Vol. 12, 2019, 3799. https://doi.org/10.3390/ma12223799
[8] Junhao Z, Xiuquan C, Qinxiang X, Chang Y. "Strengthening effect of laser shock peening on 7075-T6 aviation aluminum alloy," *Advances in Mechanical Engineering*, Vol. 12, No. 8, 2020, pp. 1-13. https://doi.org/10.1177/1687814020952177
[9] Ruslan K, S¨oren K, Nikolai K. "Identification of Johnson-Cook material model parameters for laser shock peening process simulation for AA2024, Ti–6Al–4V and Inconel 718," *Journal of Materials Research and Technology*, Vol. 28, 2024, pp. 1975-1989. https://doi.org/10.1016/j.jmrt.2023.11.168
[10] Frija M, Fathallah R, Ben Fkih L, "Modeling of the superficial Laser Shock Peening treatment Process: Application on a Titanium aircraft turbine engine blade," *Applied Mechanics and Material*, Vol. 62, 2011, pp. 85-94. https://doi.org/10.4028/www.scientific.net/AMM.62.85
[11] Kristina L, Thomas JS, Michael EF, "Finite Element Analysis of Laser Peening of Thin Aluminum Structures," *Metals*, Vol. 10, 2020, 93. https://doi.org/10.3390/met10010093
[12] Ivetic G, "Three-dimensional FEM analysis of laser shock peening of aluminium alloy 2024-T351 thin sheets," *Surface Engineering*, Vol. 27, No. 6, 2011, pp. 445-453. https://doi.org/10.1179/026708409X12490360425846
[13] Praveenkumar K, Sudhagara Rajan S, Swaroop S, Geetha M, "Laser shock peening: a promising tool for enhancing the aeroengine materials' surface properties," Surface Engineering, Vol. 39, No. 3, 2023, pp. 245-274. https://doi.org/10.1080/02670844.2023.2206186
[14] Junhao Z, Xiuquan C, Qinxiang X, Chang Y, "Strengthening effect of laser shock peening on 7075-T6 aviation aluminum alloy," *Advances in Mechanical Engineering*, Vol. 12, No. 8, 2020, pp.1-13. https://doi.org/10.1177/1687814020952177
[15] Calvin S, Arivarasu M, Sathya S, Praveenkumar K, Arivazhagan N, Muktinutalapati NR, Badirujjaman S, Basudev B, "Effect of Laser Shock Peening without Coating on Grain Size and Residual Stress Distribution in a Microalloyed Steel Grade," *Crystals*, Vol. 13, 2023, 212. https://doi.org/10.3390/cryst13020212
[16] Charles SM, Tao W, Lin Y, Graham C, Yiu WM, "Laser shock processing and its effects on microstructure and properties of metal alloys: a review," *International Journal of Fatigue*, Vol. 24, 2002, pp.1021-1036. https://doi.org/10.1016/S0142-1123(02)00022-1
[17] Jiaxuan C, Zhongyi C, Zhandong W, Hongqiang Z, Zhenlin C, Liuhe L, Ying L, Peng P, Wei G, "Effects of heat treatment combined with laser shock peening on wire and arc additive manufactured Ti17 titanium alloy: Microstructures, residual stress and mechanical properties," *Surface & Coatings Technology*, Vol. 396, 2020, 125908. https://doi.org/10.1016/j.surfcoat.2020.125908
[18] Nan L, Qiang W, Wenjuan N, Peng H, Nan G, Shenao L, "Microstructure and wear behaviors of 17-4 PH stainless steel fabricated by laser cladding with post laser shock peening treatment," *Wear*, 2024, pp. 538-539. https://doi.org/10.1016/j.wear.2023.205207
[19] Abdulhadi K, Evan TS, Saeed MF, Ahmed AA, Abdul AH. Kadhum ABM, "Effect of Multipath Laser Shock Processing on Microhardness, Surface Roughness, and Wear Resistance of 2024-T3 Al Alloy," *The Scientific World Journal*, Vol. 2014, 2014, Article ID490951, 6 pages. https://doi.org/10.1155/2014/490951
[20] Ruslan K, Sören K, Nikolai K,"Identification of Johnson-Cook material model parameters for laser shock peening process simulation for AA2024, Ti–6Al–4V and Inconel 718," *Journal of Materials Research and Technolog*, Vol. 28, 2024, pp. 1975-1989. https://doi.org/10.1016/j.jmrt.2023.11.168
[21] Nobre JP, Polese C, Staden SNV, "Incremental Hole Drilling Residual Stress Measurement in Thin Aluminum Alloy Plates Subjected to Laser Shock Peening," *Experimental Mechanics*, Vol. 60, 2020, pp. 553-564. https://doi.org/10.1007/s11340-020-00586-5
[22] Ballard P, "Residual stresses induced by rapid impact. Application to laser shock," PhD thesis, Ecole Polytechnique X, France 1991.
[23] Song H," Experimental and numerical analysis of residual stress distribution induced by laser shock in aluminum alloys," Doctoral thesis, École Nationale Supérieure d'Arts et Métiers, France 2010.
[24] Cellard C, "Study of laser shock on Ti-17 titanium alloy: Application to thin plates," PhD thesis, University of Technology of Troyes, France 2010.
[25] Warren AW, Guo YB, Chen SC," Massive parallel laser shock peening: Simulation, analysis, and validation," *International Journal of Fatigue*, Vol. 30, No. 1, 2008, pp. 188-197. https://doi.org/10.1016/j.ijfatigue.2007.01.033
[26] Bikdeloo R, Farrahi GH, Mehmanparast A, Mahdavi SM, "Multiple laser shock peening effects on residual stress distribution and fatigue crack growth behaviour of 316L stainless steel," *Theoretical and Applied Fracture Mechanics*, Vol. 105, 2020, 102429. https://doi.org/10.1016/j.tafmec.2019.102429
[27] Pan X, Zhou L, Wang C, Yu K, Zhu Y, Yi M, Wang L, Wen S, He W, Liang X, "Microstructure and residual stress modulation of 7075 aluminum alloy for improving fatigue performance by laser shock

peening," *International Journal of Machine Tools and Manufacture*, Vol. 184, 2023,103979. https://doi.org/10.1016/j.ijmachtools.2022.103979

[28] Johnson GR, Cook WH, "A Constitutive Model and Data for Metals Subjected to Large Strains, High Strain Rates and High Temperatures," Proceedings, 7th International Symposium, Ballistics, The Hague,19-21 April 1983, pp. 541-547.

[29] Johnson GR, Cook WH,"Fracture characteristics of three metals subjected to various strains, strains rates, temperatures and pressures," *Engineering fracture mechanics*, Vol. 21, 1985, pp. 31-48. https://doi.org/10.1016/0013-7944(85)90052-9

[30] ABAQUS, Inc, ABAQUS User's Manual, Ver, 6.7, Karlsson and Sorensen Inc, 2014.

[31] Mounir F,"Prediction of the reliability of multicyclic fatigue resistance of mechanical components treated by laser shock," Doctoral thesis, École Nationale d'Ingénieurs de Monastir, Tunisia 2018.

[32] Fabbro R, Fournier J, Ballard P, Devaux D, Virmont J, "Physical study of laser-produced plasma in confined geometry," *Journal of Applied Physics*, Vol. 50, No. 3, 1990, 775. https://doi.org/10.1063/1.346783

[33] Zhang W, Yao YL, Noyan IC,"Microscale laser shock peening of thin films, Part 1: Experiment, Modeling and Simulation," *Journal of Manufacturing Science and Engineering. Transactions of the ASME*, Vol. 126, No. 1, 2004, pp. 10-17. https://doi.org/10.1115/1.1645878

[34] Hirano K, Sugihashi A, Imai H, Hamada N," Mechanism of anisotropic stress generation in laser peening process," In: Proceedings of Icaleo conference, Miami, USA, 2006.

[35] http://62.108.178.35:2080/v6.14/books/stm/default.htm?startat=ch01s05ath12.html